InnoVationinfo

Journal of
Biomedical Research and Reviews

ISSN: 2581-7388
Volume 4: 1
J Biomed Res Rev 2021

Effect of High- and Low-Pressure Circulation Patterns above Mid-Latitudes on the Incidence of SARS-COV-2 across Wider European Sector during Early Spring 2020

Marek Kučera*[1]

Athanasios Kyriazopoulos[2]

Peter Kučera[3]

[1]*Department of Geography and Geoecology, Faculty of Science, Charles University in Prague, Czechia*

[2]*Chief Translator, Radnet Editions, Athens, Greece*

[3]*Mobile Engineer, Radiodetection, Western Dr, United Kingdom*

Abstract

The presented paper evaluates SARS-CoV-2 in relation to high-, neutral and low- pressure zones above mid-latitudes (North Atlantic Oscillation/NAO and Arctic Oscillation/AO phases) and simultaneous effects of 8 meteorological elements across Europe and its wider region during early spring 2020. Data of national daily incidence of SARS-CoV-2 (for 86 countries and dependent territories) were correlated with daily values of 8 meteorological elements in 137 representative cities for 3 periods before an incidence day corresponding to incubation time of SARS-CoV-2. Period 0-9th day represented negative, period 5-14th day neutral and period 10-19th day positive NAO/AO pattern. Incubation time in last period was shifted, because some cases were linked to longer waiting for results of testing or in later course of SARS-CoV-2. Patterns linked with high-, neutral and low- pressure zones above mid-latitudes were outlined. Results have shown that, during the high-pressure pattern above mid-latitudes, lower precipitation, higher pressure, weaker wind, higher sunshine, higher diurnal temperature range (higher maximum and lower minimum temperatures) were very unfavorable for incidence of SARS-CoV-2 (more cases) and that, during the low-pressure pattern above mid-latitudes, lower pressure, higher wind and less than NAO+ lower precipitation, higher sunshine and higher diurnal temperature range (mainly higher maximum temperatures) were unfavorable. For comparison these results were outputted with circulation conditions NCEP/NCAR reanalysis. During NAO+, precipitation and wind/minimum temperatures, precipitation and pressure; during NAO-, minimum temperatures, wind and sunshine/maximum, minimum and average temperatures, precipitation, sunshine and snow cover have the most simultaneous same/opposite effects.

Keywords: SARS-COV-2, Weather, Correlation, Europe, Spring-2020.

Introduction

The 2019–21 coronavirus pandemic is an ongoing pandemic, caused by severe acute respiratory syndrome coronavirus 2 (SARS-CoV-2). The outbreak was identified in Wuhan, China, in December 2019, declared to be a Public Health Emergency of International Concern on 30 January 2020, and recognized as a pandemic on 11 March 2020 (WHO, 2020a, b) [1,2].

The usual incubation period (the time between infection and symptom onset) ranges from one to 14 days; it is most commonly five days [3].

Article Information

Article Type: Research Article

Article Number: JBRR-145

Received Date: 11 December, 2020

Accepted Date: 04 February, 2021

Published Date: 11 February, 2021

***Corresponding author:** Marek Kučera, Department of Geography and Geoecology, Faculty of Science, Charles University in Prague, Albertov 6, 128 4, Czechia. Tel: +421950889368; E-mail: marekkucera556@gmail.com

Citation: Kučera M, Kyriazopoulos A, Kučera P (2021) Effect of High- and Low-Pressure Circulation Patterns above Mid-Latitudes on the Incidence of SARS-COV-2 across Wider European Sector during Early Spring 2020. J Biomed Res Rev Vol: 4, Issu: 1 (01-18).

The aim of this study is to give a comprehensive picture of the 8 meteorological elements' effect on the incidence of SARS-CoV-2 during the main circulation patterns in the Euro-Atlantic area, in the northern hemisphere respectively (NAO-/AO- versus NAO+/AO+). The goal is to detect significant differences between pre-dominant high pressure phase above mid-latitudes (NAO+/AO+) and pre-dominant low pressure phase above mid-latitudes (NAO-/AO-) for better understanding the effect of main circulation patterns on the next behavior of SARS-CoV-2.

Recent studies about effect of weather on the incidence SARS-CoV-2

SARS-COV-2 is a relatively large virus with a size of about 1–2 nm from a group of enveloped virus family with a positive-sense single-stranded RNA. The virus is transmitted by coughing and sneezing through direct contact with the infected people (respiratory droplets) and infected surfaces (can survive for hours outside the host). SARS-CoV-2 general signs and symptoms are fever, cough and breath problems. In severe cases, infection evolves to pneumonia, serious respiratory problems and, on rare occasions, it can be deadly, mainly for older people [4].

While influenza virus is linked to cold weather and peak of flu season is reached in the middle of winter, it is still a question how SARS-CoV-2 is linked to weather. Widespread testing and dependence between cooler countries in the north may cause, that number of confirmed SARS-CoV-2 cases between cooler northern and warmer-humid southern regions is different. However, more southern countries have realized large-scale testing and the number of positive to SARS-CoV-2 cases (per capita) are lower than in northern climate [5].

Sajadi et al. [6] predict Potential Spread in connection with Seasonality for SARS-CoV-2, using climate data from cities with prominent spread of SARS-CoV-2. Authors predict where are the most likely higher risks of spreading of SARS-COV-2. To date, SARS-CoV-2, has created a significant community spread in big cities in the countries along a narrow west east regions crudely along the 30-50° N latitude with similar weather conditions (average temperatures of 5-11°C, absolute humidity (4-7 g/m3) and low specific (3-6 g/kg)). Significant predictors for spreading of a virus are mainly population proximity and interaction of people through travel.

Tang et al., [7] have researched the survival of the airborne human coronavirus HCV/229E. This virus was used by authors as a representative or surrogate of respiratory coronary viruses and it was examined under various temperature and relative humidity conditions. Authors demonstrated that under such conditions, the virus has a half-life of 27 / 67 / only 3 hours at 30% / 50% / 80% humidity. Here is an evidence, that near higher relative humidity, half-life of virus has considerably shorter time of survival. When the temperature drops as 6°C, HCV/229E half-life is redoubled to 6 hours at 80% humidity. Similar results have been found for seasonal flu [8]. It is assumed that this severe effect on prolonging the virus's half-life is linked to the spreading of the SARS-CoV-2 during to low-temperature and high-humidity pattern of weather [4].

Wang et al. [9] researched the influence of air temperature and humidity on the transmission of SARS-CoV-2. Meteorological data for 100 Chinese cities with more than 40 cases were used. According to the study, the arrival of humid summer season could significantly diminish the transmission of the SARS-CoV-2.

Ma at al. [10] explored the association between SARS-CoV-2 deaths and weather parameters (temperature and humidity) in 2299 SARS-CoV-2 related deaths. Both meteorological elements are considered as important factors for increasing/decreasing SARS-COV-2 mortality.

Chan et al. [11] investigated on the effect of temperature and humidity on SARS-CoV-2. Authors used as target group of viruses HKU39849 strain. Facilitations of SARS-CoV-2 transmission were linked with lower temperature and dry conditions.

Xiao et al. [12] found that big air pollution also has an effect on the impacts of SARS-CoV-2. An increase of only 1 μg/m3 in PM2.5 brings a 15% increase in the SARS-CoV-2 death rate at the level of significance 0.05. Results are statistically significant and robust to secondary and sensitivity analyses.

Using data on local transmissions until the 23rd of March 2020, Araujo and Naimi [13] in a preprint article developed an ensemble of 200 ecological niche models to project monthly variation in climate suitability for spread of SARS-CoV-2 throughout a typical climatological year. Although cases of SARS-CoV-2 are reported all over the world, most outbreaks demonstrate a pattern of clustering in cooler and drier regions. The predecessor SARS-CoV-1 was linked to similar – dry and cold climate conditions. Authors expect asynchronous seasonal global outbreaks unless current trends of spreading SARS CoV-2 will be continuing. Models have shown that temperate cold and humid climates are more favorable to spread of the virus, whereas tropical hot and arid climates are less favorable. Nevertheless, model uncertainties are still high in the regions of sub-Saharan Africa, Latin America and South East Asia. Unsuitable climates can cause quick destabilization and reducing capacity of the virus.

Correspondence of Brassey et al. suggests that cold and dry conditions may influence the transmission of SARS-CoV-2. Authors gave a summary of evidences from unpublished papers till 22. March 2020 [14]:

- A cross-sectional study found that every 1°C of increase in the minimum temperature led to a decrease in the cumulative number of cases by 0.86.

- A modeling study suggested a transitory reduction of incidence in spring and summer period and subsequently increase during the winter period 2020-2021.

- Another modeling study found that the current spread preferences are cool and dry conditions. 2002-3 SARS-CoV-1 outbreak was linked to similar weather conditions.

Conclusions and predictions of these studies have high

uncertainty (their results are potentially biased because of uncontrolled confounding).

- Next two studies announce that daily mortality of SARS-CoV-2 is positively correlated with diurnal temperature range (DTR) but negatively correlated with relative humidity. Temperature and relative humidity are likely to contribute a maximum of 18% of the variation in transmission. Every 1°C increase in temperature / 1% increase in relative humidity lowered the R by 0.0383 / 0.0224.

- A very recent modeling study investigated the relationship between temperature and predicted the number of cases. Lower temperatures were worse for incidence of SARS-CoV-2 than were higher ones.

Lin et al. [15] investigated to identify factors involved in the emergence, prevention and elimination of SARS-CoV-1 in Hong Kong from 11 March to 22 May 2003. A structured multiphase regression analysis has shown the potential effects of weather, time and interaction effect of hospital infection on severe acute respiratory syndrome. In colder days during the epidemic, the risk of increased daily incidence of SARS-CoV-1 was 18.18-fold (5.6-58.8 at the level of statistical significance 0.05) higher than in warmer days. Naturally decrease during the epidemic might by an average of 2.8 the total daily new cases every 10 days. The authors considered SARS-CoV-1 transmission to be dependent on temperature changes during the climate year and on the multiplicative effect of hospital infection. SARS-CoV-1 retreated naturally during the further development of the epidemic.

Tan et al. [16] have found a significant correlation between the SARS-CoV-1 cases and the air temperature seven days before the incidence and the seven-day time lag corresponded well with the well-known incubation period. The optimum air temperature linked with the SARS-CoV-1 cases (and its encourage virus growth) was from 16 to 28°C. A sharp decrease (and too rise) of air temperatures related to the cold spell led to an increase of the SARS-CoV-1 cases - human immune system is influenced by cold weather. There are some evidences that a higher possibility for SARS-CoV-1 to reoccur is during the spring more than the autumn / winter.

Gardner et al. [17] studied a background of Middle East respiratory syndrome coronavirus (MERS-CoV) from January 2015 to December 2017. To find linkages between primary MERS-CoV cases and previous weather conditions within the incubation period (2 weeks) in Saudi Arabia a case-crossover design using invariable conditional logistic regression was used. The full case dataset (1191 cases) was reduced to representative group most likely to represent spillover transmission from camels (446 cases). In research, meteorological data from localities closest to the largest city for each Saudi region were used (daily maximum, minimum and mean temperature (in °C), relative humidity (in %), wind speed (in m/s), and visibility (in m). Lowest temperature (Odds Ratio=1.27; 1.04-1.56 at the level of statistical significance 0.05) and humidity (Odds Ratio=1.35; 1.10-1.65 at the level of statistical significance 0.05) were linked with incidence of MERS-CoV 8-10 days later, high visibility 7 days later (Odds Ratio=1.26; 1.01-1.57 at the level of statistical significance 0.05) and wind speed 5-6 days later.

Given the previous associations between viral transmission and humidity and temperature across which the majority of the SARS-CoV-2 cases have been observed until the present date, that lower humidity and lower temperatures are unfavorable for incidence of SARS-CoV-2. If SARS-CoV-2 is relatively sensitive to these types of weather, then it could be applied to optimize the to SARS-CoV-2 mitigation strategies [5]. The provision of protective gear is also a very important factor for the prevention of SARS-CoV-2 infection. Other circulating viruses, such as flu copy a seasonal effect, and for that reason co-infection rates will have decline trend, which may have effect on death rate [14].

The role of airborne transmission in SARS CoV-2 infection and the role of masks in mitigating transmission in relation to meteorological elements

The highly infectious nature of SARS-CoV-2 has been carefully investigated by the scientific community during the first year of the virus' appearance.

A review of the available evidence on the viral dynamics of SARS-CoV-2 in the upper respiratory tract and an attempt of determining a timeline for the infection based on molecular and viral culture can be found in the work of Tirupathi et al. [18]. Mild to moderate cases have shown a peak of viral load in the 1st week of illness, a delayed viral load peak in the 2nd week in severe disease compared to mild disease which has viral load peaks in the 1st week of infection [18-21]. Older and male patients experienced longer duration of disease, delayed admission to hospital after illness onset, invasive mechanical ventilation and corticosteroid treatment [22-24]. Higher concentration of ACE-2 receptors in adult airways was crucial [25].

Liu et al. (2020) moreover suggested contagiousness to at least 1-week after "clinical recovery" (while most studies have demonstrated virus culture isolation only under 10 days) [20].

The magnitude, persistence and durability of the immune response, according to Tirupathi et al., vary due to various factors that influence protection [18].

In their next article, Tirupathi et al. investigated airborne transmission of SARS-CoV-2 with emphasis on the importance of masks in mitigating transmission [26]. One of the results of the research, i.e. that in the USA, 66.7% of air samples taken from researched hospital hallway carried virus-containing particles, should raise a lot of questions about the mechanisms of spreading of a virus through particles in the air [27,28].

Experimental data suggest that SARS-CoV-2 may be transmitted by aerosols (the so-called airborne transmission) even in the absence of aerosol-generating procedures (e.g. intubation or noninvasive positive pressure ventilation) [29].

Normal speaking also produces thousands of oral fluid

droplets with a broad size distribution (ca. 1 μm to 500 μm) [30].

Airborne transmission is attributed mainly to infectious droplet nuclei produced by the desiccation of suspended droplets and defined as 5 μm or smaller in size [31]. A susceptible host can be close to a patient or at a distance from a patient, and, as in the case of SARS-CoV-1, the 2009 H1N1 influenza pandemic and MERS-CoV, possibilities of spreading of the virus were found for a) droplet bourne route (transmitted by medium or large droplets for short distances); b) short-range airborne route (transmitted by aerosols for middle distances); c) long-range aerosols route (transmitted by aerosols for long distances) and d) fomite route (transmission from surfaces) (Wei and Li, 2016).

Despite of many critic studies (increased touching of face, questionable effect of masks in public spaces, etc.), according to Tirupathi et al. universal masking should be associated with other favorable practices like temperature checks and symptom screening on a daily basis to enjoy the maximal benefit from masking (99.98%, 97.14%, and 95.15% efficacy for N95, surgical, and homemade masks respectively according to Ma et al.; Powered Air-Purifying Respirators (PAPRs) are even better, but they present disadvantages such as high cost and difficult maintenance, according to Brosseau et al. in comparison to surgical, and homemade masks respectively. Personnel in hospitals should use gloves, coats or eyes protection (prevalence of asymptotic infection within population is only around 2%, whereas among confirmed cases it is around 20-50%) [26,32,33].

"In fact, more contamination was found on the outer surface of the masks when compared to the inner surface" [34]. Therefore, it is very important to decontaminate the mask (including hand hygiene) before reusing it.

Shao's et al. results showed that the design of ventilation is critical for reducing the risk of particle encounters. Inappropriate design can create local hot spots by favoring particle deposition that cause surface contamination [7]. Surface contamination strongly correlate with breathing depth. The key ventilation-associated recommendations are described in the work Morawska et al. [35].

Aerosol transmission and inactivation of infectious influenza A viruses depend on humidity levels [36]. The shrinking of respiratory droplet size when humidity drops from 90% to 10% in 10 min explains the 2.4-times increase in virus concentration; therefore, a high humidity indoors to prevent the spreading of COVID-19 is highly recommended.

The filtering capacity, and hence the level of protection against pollutants and pathogens, depends on the materials used and the engineering design [37-42].

SARS-CoV-2 has a size ranging from 60 to 140 nm, smaller than bacteria, dust, and pollen. Therefore, masks and respirators made of materials with larger pore sizes, such as cotton and synthetic fabric, will not be able to effectively filter these tiny droplets [37]. Materials with much smaller pore sizes are, on the contrary, more effective. Similarly, masks made of or coated with water-resistant material are more effective against droplets and fluid spills. This is the reason for the success of N95 respirators and surgical masks [43]. The efficiency of household materials (cotton fabrics, clothing, silk, tissue paper, kitchen towels, pillowcase, and tea cloths), as well as of commercial masks (with original names) are described in detail in Ming Hui et al., 2020.

O' Kelly et al. found that when fabrics were layered, a higher percentage of ultrafine particles were filtered. The average filtration efficiency of single layer fabrics and of layered combination was 35% and 45%, respectively. Non-woven fusible interfacing, when combined with other fabrics, could add up to 11% additional filtration efficiency [44].

Neuphane et al. found that PM10 filtration efficiency dropped by 20% after the 4th washing and drying cycle [45].

In relation to dry conditions, the efficiency of masks should be associated with the adsorption of their material, their adhesion and the gaps through which the virus might penetrate under the mask [28,46,47]. Almost dry weather, adsorption on the cover of masks and adhesion within many types of fabrics should be increased. Dry (and sunny) conditions similarly such as drying of material are worsening the quality of masks, as we have mentioned before [48].

The question is how cold conditions during winter months affect the temperature comfort of the carrier of the mask – here, well-made homemade masks should be relatively successful (with higher efficacy than usual) to reduce stress related with temperature differences between body surfaces under and outside of masks, in opposition to surgical or N95 masks.

Risk of mechanic transition of virus under mask is higher during windy or during combinations of uncomfortable weather conditions (mechanic shifts of the mask, hands on the face).

It is generally admitted that intense sunshine should be linked with loss of mask quality [49].

Lower visibility and foggy anticyclonic conditions during winter season should be associated with higher particles of air pollution, which means higher need for decontamination of the masks.

According to Volz, the new "British" variant of SARS-CoV-2 has a transmission advantage of 0.4 to 0.7 in reproduction number compared to the previously observed strain (2.5 - 3 according to Liu et al.); therefore, the importance of all the above-mentioned factors is even more crucial [50,51].

Main circulation patterns in the mid-latitudes (North Atlantic Oscillation/NAO and Arctic Oscillation/AO phases)

Seasonal climatic anomalies manifest themselves over large geographical regions. Some areas appear cooler and drier, whereas others, hundreds to thousands of kilometers away, warmer and wetter. These parallel structures with opposite phases and manifestations in climatology are referred to as teleconnections. Most often, they are determined using one point correlation maps, comparing

the correlations of the height of the grid field points of the pressure level of 500 hPa and the reference point. Low-frequency oscillations are also reflected in the ground pressure field. After depicting air pressure anomalies at sea level, the ground air pressure dipole is visible [52]. A total of 13 modes have been identified that affect the northern hemisphere climate. The NAO (AO) mode is the only one of all modes having expression in Europe throughout the year, the other 3 main modes - EA, EU2 and EU1, are only visible in selected seasons. Among teleconnections we can include Southern Oscillation (ENSO) too, but it has no significant manifestations in Europe, it is considered with AO to be the most extensive oscillation affecting the climate on Earth.

The magnitude of the pressure gradient between the Arctic and moderate latitudes is closely related to the evolution of the polar vortex and the nature of the jet stream. In meteorology, this magnitude is linked with two major oscillation modes occurring above the northern hemisphere: Arctic Oscillation (AO) and North Atlantic Oscillation (NAO). AO is clearly identifiable in pressure fields (especially in winter) throughout the northern hemisphere, while the NAO is its equivalent to the Euro-Atlantic area. 90% of the oscillations are interconnected. If the AO and NAO indices both show negative values (negative phase), this results in a weaker and less pronounced polar vortex and a weaker and meandering jet stream. Stronger polar vortex and more zonal running and strong jet the stream, on the other hand, is associated with the positive phase of AO and NAO. Each phase has its typical manifestations in pressure, temperature and precipitation fields in individual regions, including Europe [53-57].

The NAO describes in a meridional direction the transfer of atmospheric masses between the subtropical region in the Azores Pressure Area and the sub-polar in the Icelandic Pressure Area. It affects both seasonal and interdecadal variability in global circulation [53] and is the only oscillating mode to show statistically significant links with meteorological characteristics in Europe throughout the year. According to Hurrell et al. [52] the area of influence of the NAO extends from the east of the USA to Siberia in the zonal and from the Arctic to the subtropical Atlantic in the meridional direction.

There are two types of situations: type A - equivalent of negative phase: NAO-/AO- (weakening of pressure formations in the North Atlantic) and type B - equivalent of positive phase: NAO+/AO+ (more developed pressure units). The distribution of pressure units over the Atlantic varies considerably in winter and summer - in the summer, the Azores High (the first NAO Action Center) dominates, which also extends northwards due to the shift of the intertropical convergence zone to the north. On the contrary, it weakens and shifts to the south during winter, with Icelandic Low dominating the Euro-Atlantic area (second NAO action center). Differences in air pressure deviations between the positive and negative NAO phases in action center areas are over 15 hPa. Significant changes in atmospheric circulation remodeling occur when the NAO index exceeds +1 or -1 [53].

During the positive phase of the NAO, anomalously higher air pressure occurs west to southwest of the coast of Europe in combination with anomalously low air pressure in the Arctic Atlantic. The flow generated by the rotation of pressure formations is intensified by a larger pressure gradient, causing a more pronounced western flow at moderate latitudes over (North) Atlantic and (Northern) Europe, a southern flow over the east coast of the US and north over western Greenland and Canada. The western flow brings warmer and damper sea air to Europe in winter and causes milder winter, while the northern flow from the Great Lakes to the north and northeast causes more waves of cold and blizzards. In the negative phase, the situation is reversed: the pressure formations above Iceland and the Azores are anomalously weakened (shallower Iceland low and less robust Azores high). A weak meridional pressure gradient causes a weak western flow, so much humid and warm ocean air does not get above Europe in winter, a suitable situation for meridional air mass transfer occurs and potential invasions of Arctic and Siberian air. With the extremely low oscillation index, seasonal Greenland High increases, bringing above-average air temperatures in Canada, the United States and Greenland, but significant cold air inflows over Europe. The following patterns of correlation of the NAO index with the most important meteorological elements - precipitation, air temperature and pressure field distribution [58] were identified:

1.) Summer: During the positive phase of the NAO, there is a robust pressure high above the British Isles, extending from the Azores to Scandinavia, with a center in Scotland and Northern Ireland. There is a deep low-pressure area above Greenland, and a low-pressure field extends over the Mediterranean. On the contrary, during the negative phase of the NAO, anomalous high-pressure spreads over the area of Iceland and Greenland, and areas of mid- and subtropical latitudes from North America over the Atlantic to mid-latitudes of Europe and the Mediterranean report negative surface pressure anomalies. The largest negative pressure anomalies are achieved in northern Germany and Denmark [59]. Positive correlations with precipitation are achieved during the summer and positive NAO phases in the British Isles, Benelux, north of France, Germany and Poland to the Eastern Carpathians, the south of Scandinavia and the Baltic Sea. The robust high pressure above Northwest Europe during the NAO+ (Action Center) causes a flow of cooler and drier air over the continent, which has a stabilizing effect on temperatures and precipitation in Central Europe. Negative correlations with precipitation have been confirmed across the Mediterranean, from Spain to Turkey, with the highest values in the Adriatic and the Balkan. The penetration of cooler air from the northwest generates numerous precipitations and low temperatures - mainly above the Balkans, Italy, Turkey, to Israel and Egypt. On the contrary, the robust pressure above the British Isles brings, in addition to drought, above-average temperatures on the British Isles, and from west and north-west coasts of Europe to the Baltic. During the negative NAO phase, temperature and precipitation responses are reversed.

2.) Winter: The different nature of winters is largely related to the tracking of Atlantic cyclones in winter. During

the winter when the polar vortex is locked above the sub-polar region and the zonal flow reaches high levels, the low-pressure action center is located more northerly on the Greenland - Iceland axis. The deep Icelandic low travel across Europe by northern tracks - over the British Isles and Scandinavia, at most the coast of the North Sea and the Baltic Sea. Europe (except the British Isles and Scandinavia) is on the front of the quasi-stationary deep low pressure zone in the warm, predominantly southwestern, during the winter NAO + phases, while stormtrack is shifting from the Island-British Isles axis to the north of Europe. The activity of Mediterranean cyclones is minimal - in the Mediterranean there is dry and relatively cold weather (thanks to clear anticyclonic nights). The northernmost and, in particular, the more robust regions of the Azores high reach western, southern but also central Europe more often than usual during these phases. During the negative phase the situation is reversed - the stormtracks are due to the extensive meanders of the polar and arctic front and weakened zonal air transport curved over the Mediterranean. Due to the disintegration of the polar vortex, the jet-stream is forced to the south, generating low pressure over lower latitudes (southern, moderate and subtropical regions). The low pressure over the Mediterranean and the high pressure over Scandinavia and the northern half of Europe, together with the more pronounced Siberian anticyclone, then create suitable conditions for invasions of Arctic or dry and cold Siberian air over Europe (the Mediterranean pressure lows "pulling" cold air towards them). Pressure field such this, typical for NAO-phases, is associated with cyclonic weather with higher temperatures and higher rainfall totals over the Mediterranean, and drier and cold conditions over the northern half of Europe. In winter, correlations of the NAO index with temperatures and precipitation have a stronger zonal pattern than in summer. A clear signature of the positive NAO phase on air temperatures, precipitation, as well as the total pressure field and flow is present from North America to eastern Siberia and is associated with overall warming in Siberia and cooling in eastern Canada and from subtropical to tropical latitudes.

Data and Methods

Three types of data are used in the analysis: daily meteorological data from International Exchange Network (covered by World Meteorological Organisation); daily incidence of to SARS-CoV-2 measured by World Health Organisation and NCEP/NCAR Reanalysis from Physical Sciences Laboratory, NOAA. We have focused to evaluate and quantify effect weather to SARS-CoV-2 for countries in wider European region. It comprises 86 countries and dependent territories and 137 cities in 13 main examined regions (Figure 1 and Table 1) in Europe, Africa, Asia and North America. All days for the period from 8. February to 7. April 2020 were filtered to whether they fall under compact period of incidence SARS-CoV-2, with starting day with minimally 25% of value of maximum incidence. Then was chosen the 3 periods from International Exchange Network for representative meteorological stations in these countries (overall 137 localities) and correlated with each other.

We used for this analysis meteorological data of: TG – average temperature (°C), TX – maximum temperature (°C), TN – minimum temperature (°C), RR – 24-hours precipitation (mm), PP – air pressure (Hpa), WW – average daily wind speed (km/h), SS – sunshine duration (h) and snow cover (cm). From pairs of daily health and previously meteorological data were computed Spearman correlation ranks. From these data were outlined correlation matrix and correlation maps (for every city, with significance at level 0.10) for every from 8 meteorological elements and 3 periods of incubation time. We were chosen 3 periods of an incubation time as an input of meteorological data to correlation analysis: 10-19 days before an incidence, 2. 5-14 days before an incidence and 1, 3. 0-9 days before an incidence.

Mean date of meteorological data before an incidence was for the 1st period 16. March, for 2nd period 21. March and for 3rd period 26. March. These dates were closer to end of incidence time series, because count of the stations/countries with longer outbreak was decreasing by time. Dates falling under interval of meteorological data before an incidence (middle position of 10 day window) was from 7. March to 22. March for 1st period, from 12. March to 27. March for 2nd period and from 17. March too 2. April 2020 for 3rd period. (We neglected Bahrain station, where outbreak have begun very early (25% threshold was reached in 26. February and meteorological data were used from date 8. February – periods would be extended for 3.5 ago in comparison to results). These periods relative clearly fitted with strong NAO+/AO+ phase with NAO index over 1.0 during the 1st period, neutral transient phase of NAO/AO during the 2nd period and strong NAO- or relative strong AO neutral phase with NAO index under -1.0 during the 3rd period. In this positioning, effect main circulation phases above mid-latitudes to SARS-CoV-2 in 3 incubation time periods could be examined. Incubation time was in last period shifted, because some part of cases was linked with longer waiting for results of testing or in later course of SARS-CoV-2, therefore results could better fit to real incubation time before a day of results of tests.

For identified positive, negative and neutral phase of NAO/AO in outputs were computed NCEP/NCAR Reanalysis plots for verification and understanding of circulation conditions.

Spearman ranks were finally correlated to each other for findings of patterns, whose meteorological elements have a common effect on the incidence of SARS-CoV-2, with same shift or opposite shift. These computations were realized for 13 main regions.

Results and Discussion

In this chapter we evaluate the resulting nature of the spatial variability of effects 8 meteorological elements to incidence SARS-CoV-2 during 3 periods falling under incubation time and main circulation patterns. We also point to differences in incidence of SARS-CoV-22 between main circulation patterns across Europe and its wider area (especially differences between the positive and negative phases NAO/AO). On the basis of NCEP/NCAR Reanalysis

Figure 1: Up: List of 137 cities (representative meteorological stations) with their WMO CODE, date of the first day of meteo data (Weather) and incidence data (Incidence) entering to the computations and main region (Region) of cities; Down: Map of used stations (cities) within 13 main regions.

CODE	City	Weather	Incidence	Region	CODE	City	Weather	Incidence	Region	CODE	City	Weather	Incidence	Region
40990	Kandahar	8.3.	26.3.	SASIA	04250	Nuuk	2.3.	20.3.	ARCTIC	08512	Ponta Delegac	4.3.	22.3.	T ISL
13601	Tirana	7.3.	25.3.	BALKAN	12843	Budapest	1.3.	19.3.	C EU	78526	San Juan	10.3.	28.3.	T ISL
60369	Alger	6.3.	24.3.	N AFR	)4030/13(	Reykjavik	24.2.	13.3.	ARCTIC	41170	Doha	23.2.	12.3.	M EAST
60680	Tamanrasset	6.3.	24.3.	N AFR	43057	Mumbai	13.3.	31.3.	SASIA	15421	Bucuresti	6.3.	24.3.	BALKAN
37788	Yerevan	28.2.	17.3.	EEU/CA	42181	New Delhi	13.3.	31.3.	SASIA	22550	Arhangelsk	12.3.	30.3.	ARCTIC
11120	Innsbruck	29.2.	18.3.	C EU	42027	Srinagar	13.3.	31.3.	SASIA	27612	Moscow	12.3.	30.3.	EEU/CA
11204	Lienz	29.2.	18.3.	C EU	40841	Kerman	15.2.	4.3.	M EAST	23078	Norilsk	12.3.	30.3.	ARCTIC
11036	Wien	29.2.	18.3.	C EU	40754	Teheran	15.2.	4.3.	M EAST	29638	Novosibirsk	12.3.	30.3.	EEU/CA
37864	Baku	9.3.	27.3.	EEU/CA	40650	Baghdad	27.2.	16.3.	M EAST	26063	Sankt Petersbı	12.3.	30.3.	STORM
41150	Bahrain	8.2.	26.2.	M EAST	03969	Dublin	2.3.	20.3.	STORM	28722	Ufa	12.3.	30.3.	EEU/CA
26850	Minsk	14.3.	1.4.	EEU/CA	40180	Tel Aviv	6.3.	24.3.	E MED	34560	Volgograd	12.3.	30.3.	EEU/CA
06451	Brussels	3.3.	21.3.	W EU	16560	Cagliari	23.2.	12.3.	W MED	40394	Hail, SA	4.3.	22.3.	M EAST
78016	Bermuda	5.3.	23.3.	T ISL	16080	Milano	23.2.	12.3.	W MED	41024	Jeddah	4.3.	22.3.	M EAST
14654	Sarajevo	4.3.	22.3.	BALKAN	16289	Napoli	23.2.	12.3.	W MED	61641	Dakar	25.2.	14.3.	N AFR
15614	Sofia	24.2.	13.3.	BALKAN	16239	Rome	23.2.	12.3.	W MED	13274	Beograd	9.3.	27.3.	BALKAN
71395	Halifax	8.3.	26.3.	ECOAST	16105	Venezia	23.2.	12.3.	W MED	11813	Bratislava	28.2.	17.3.	C EU
71714	Quebec	8.3.	26.3.	ECOAST	16090	Verona	23.2.	12.3.	W MED	14015	Ljubljana	23.2.	12.3.	BALKAN
71063	Ottawa	8.3.	26.3.	ECOAST	78397	Kingston	23.2.	12.3.	T ISL	08181	Barcelona	1.3.	19.3.	W MED
71265	Toronto	8.3.	26.3.	ECOAST	40270	Amman	27.2.	16.3.	M EAST	08001	La Coruna	1.3.	19.3.	W MED
64753	Faya	2.3.	20.3.	N AFR	35188	Astana	10.3.	28.3.	EEU/CA	60030	Las Palmas	1.3.	19.3.	T ISL
14240	Zagreb	2.3.	20.3.	BALKAN	35700	Atyrau	10.3.	28.3.	EEU/CA	08221	Madrid	1.3.	19.3.	W MED
78264	Santiago de Cu	8.3.	26.3.	T ISL	38353	Bishkek	7.3.	25.3.	EEU/CA	08306	Palma de Mal	1.3.	19.3.	W MED
17609	Larnaca	28.2.	17.3.	E MED	26422	Riga	29.2.	18.3.	STORM	02049	Gallivare	24.2.	13.3.	ARCTIC
11520	Prague	2.3.	20.3.	C EU	40100	Beyrouth	23.2.	12.3.	E MED	02458	Uppsala	24.2.	13.3.	STORM
06180	Cobenhagen	23.2.	12.3.	STORM	62271	Kufra	12.3.	30.3.	N AFR	06700	Geneve	27.2.	16.3.	C EU
78486	Santo Dominc	4.3.	22.3.	T ISL	06990	Vaduz	1.3.	19.3.	C EU	06770	Lugano	27.2.	16.3.	C EU
62463	Hurghada	8.3.	26.3.	N AFR	26730	Vilnius	4.3.	22.3.	STORM	06660	Zuerich	27.2.	16.3.	C EU
62366	Cairo	8.3.	26.3.	N AFR	06590	Luxembour	1.3.	19.3.	W EU	40080	Damascus	9.3.	27.3.	E MED
26038	Tallin	25.2.	14.3.	STORM	61230	Nioro du Sa	8.3.	26.3.	N AFR	60715	Tunis	7.3.	25.3.	N AFR
63332	Bahar Dar	27.2.	16.3.	N AFR	16597	Luqa	26.2.	15.3.	W MED	17352	Adana	9.3.	27.3.	E MED
06011	Torshavn	2.3.	20.3.	STORM	33815	Chisinau	14.3.	1.4.	BALKAN	17130	Ankara	9.3.	27.3.	E MED
02978	Helsinki	24.2.	13.3.	STORM	44212	Ulaangom	21.2.	10.3.	EEU/CA	17060	Islanbul	9.3.	27.3.	E MED
02835	Inari	24.2.	13.3.	ARCTIC	13463	Podgorica	7.3.	25.3.	BALKAN	33345	Kyiv	11.3.	29.3.	EEU/CA
07510	Bordeaux	2.3.	20.3.	W EU	60155	Casablanca	8.3.	26.3.	N AFR	33393	Lviv	11.3.	29.3.	C EU
07110	Brest	2.3.	20.3.	W EU	44454	Kathmandu	6.3.	24.3.	SASIA	33837	Odesa	11.3.	29.3.	EEU/CA
07690	Nice	2.3.	20.3.	W MED	06344	Rotterdam	1.3.	19.3.	W EU	41194	Dubai	13.3.	31.3.	M EAST
07156	Paris	2.3.	20.3.	W EU	61017	Bilma	15.3.	2.4.	N AFR	03017	Kirkwall	9.3.	27.3.	STORM
37545	Tbilisi	22.2.	11.3.	EEU/CA	13588	Skopje	5.3.	23.3.	BALKAN	03166	Edinburgh	9.3.	27.3.	STORM
10382	Berlin	2.3.	20.3.	C EU	01317	Bergen	23.2.	12.3.	STORM	03772	London	9.3.	27.3.	W EU
10141	Hamburg	2.3.	20.3.	C EU	01052	Hammerfes	23.2.	12.3.	ARCTIC	03827	Plymouth	9.3.	27.3.	W EU
10870	Munchen	2.3.	20.3.	C EU	41256	Muscat	10.3.	28.3.	M EAST	72202	Miami	9.3.	27.3.	ECOAST
10738	Stuttgart	2.3.	20.3.	C EU	41780	Karachi	11.3.	29.3.	SASIA	74486	New York	9.3.	27.3.	ECOAST
08495	Gibraltar	2.3.	20.3.	W MED	41641	Lahore	11.3.	29.3.	SASIA	72520	Pittsburgh	9.3.	27.3.	ECOAST
16716	Athens	25.2.	14.3.	E MED	12566	Krakow	7.3.	25.3.	C EU	72403	Washington D(	9.3.	27.3.	ECOAST
16754	Heraklion	25.2.	14.3.	E MED	12375	Warszawa	7.3.	25.3.	C EU	38457	Tashkent	9.3.	27.3.	EEU/CA
04339	Ittoqqortoormiit	2.3.	20.3.	ARCTIC	08579	Lisboa	4.3.	22.3.	W MED					

Table 1: Up: List of 137 cities (representative meteorological stations) with their WMO CODE, date of the first day of meteo data (Weather) and incidence data (Incidence) entering to the computations and main region (Region) of cities; Down: Map of used stations (cities) within 13 main regions.

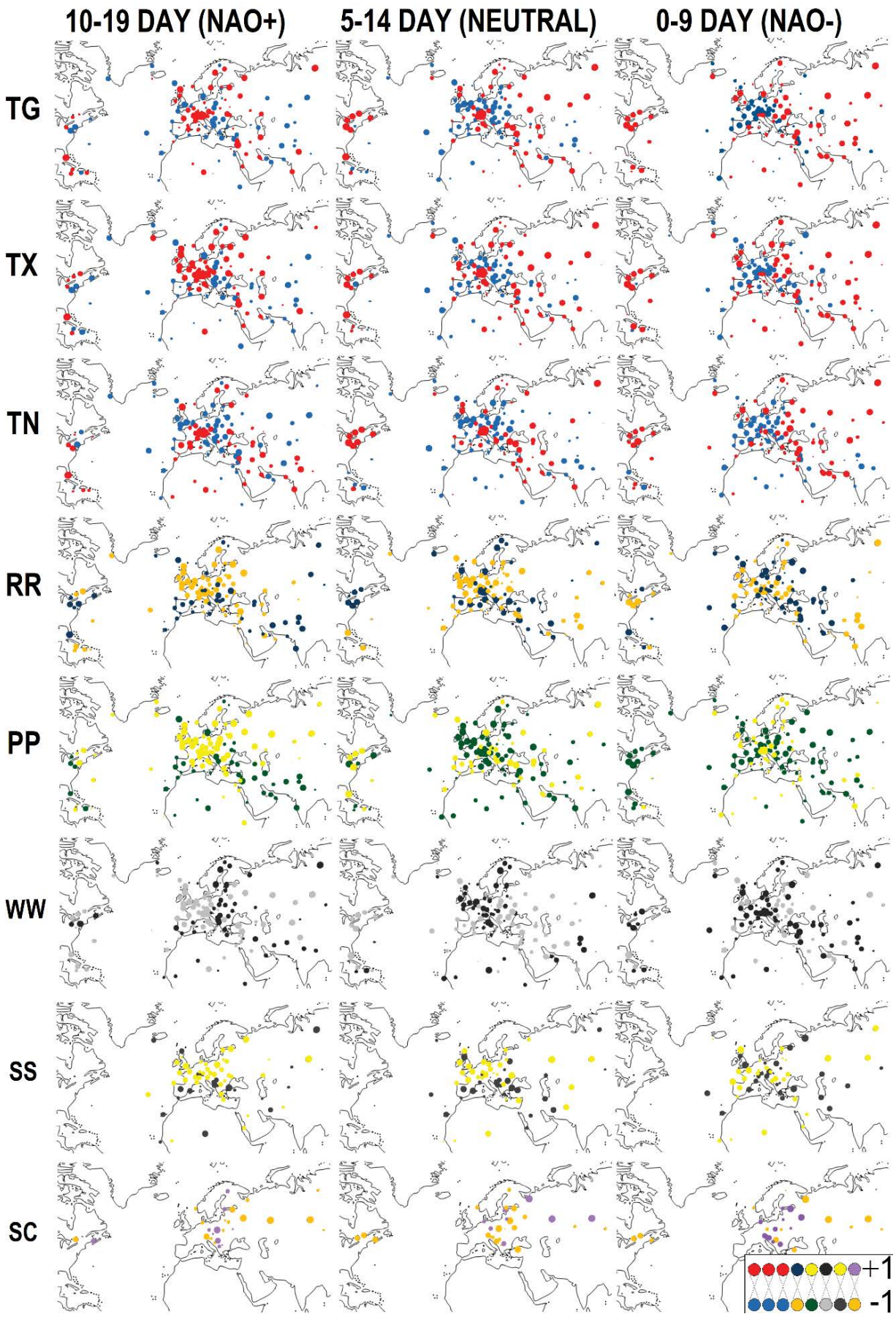

Figure 2: A: Size of correlation coefficients from table 2 for every meteorological element (same as table 2).

we evaluate the affiliation to individual phases of NAO/AO. Finally, the simultaneous same or opposite effects of meteorological elements on the incidence SARS-CoV-2 during phases are displayed using a correlation matrix and a schematic map.

Spatial distribution of effects of 8 meteorological elements on the incidence SARS-COV-2: evident impact of predominant mid-latitudes circulation patterns

Firstly, paired Spearman correlation ranks between daily value of incidence of SARS-CoV-2 and 8 meteorological elements (TG, TX, TN, RR, PP, WW, SS, SC) were computed (Table 2). Correlation coefficients were tested at level of significance 0.10. Then were outlined correlation maps for each element and 137 stations/86 countries and dependent territories (Figure 2). Values for countries and dependent territories were derived as averages from results for stations.

Results of spatial distribution of correlations computed for sea level pressure (PP) and precipitation (RR) have shown, that a substantial part of computed outlined coefficients copy the main NAO/AO pattern, when the majority of cities in mid-latitudes match the main phases of NAO/AO [52-54,56-59]. Mainly during strong NAO+/AO+ phase during 1st incubation period (10-19 days before an incidence) were thanks to AO and NAO index values above 1.0 were present strong positive/negative correlations PP/RR with SARS-CoV-2 incidence above western Europe, British Islands, Central Europe, southern and middle parts of Scandinavia, Baltic and almost all eastern Europe except for Black sea region; and on the other hand significant negative/positive correlations in Mediterranean and too above tropical, the most southeast main regions (Figure 2, PP and RR row and 10-19 days (NAO+) column). A part of investigated incidence of SARS-CoV-2 therefore was through the incubation period linked with predominant positive NAO/AO phase.

Situation during NAO-/AO- during the 3rd period (or neutral AO for better description, because AO index wasn't in minus values as NAO index) had inverse and over mid-latitudes low pressure field was preserved. More PP with SARS-CoV-2 incidence positive correlations and on the contrary, pressure over Scandinavia was height, but not with origin of Azores height with warm air, but Greenland high with cold air (northerly from southerly-shifted stormtrack in this period), and part of tropical main regions had high pressure too (subtropical heights were pushed from north to the south), were observed. RR were evenly distributed over mid-latitude area.

Considering that the behavior of coronavirus replicates the behavior of NAO and AO, we are not only able to estimate how the ground-level meteorological elements will behave during the mid-latitude predominant low- and high-pressure phases. The following subchapters deal with the observed behavior of the effects of meteorological elements on the incidence of SARS-CoV-2 during the 3 basic modes of Euro-Atlantic and North-hemispherical circulation, respectively.

SARS-CoV-2 during predominant anticyclonic weather (NAO+/AO+) in the mid-lattitudes: As we have shown in figure 2 and figure 3, the entire column for 10-19 day (NAO+) shows signs of a strong NAO +/AO+ phase with strong predominant high-pressure conditions over anticyclonic belt above mid-latitudes.

Results have shown that, during the high-pressure pattern above mid-latitudes, lower precipitation, higher pressure, weaker wind, higher sunshine, higher diurnal temperature range (higher maximum and lower minimum temperatures) were very unfavorable for incidence of SARS-CoV-2.

We can confirm previous findings, that higher drought or diurnal temperature range are very unfavorable for incidence SARS-COV-2, what means, that incidence SARS-CoV-2 is during this type of weather higher and effect of drought can be devastating [5,6,9,10,11,13,14].

Results regarding dry conditions are very similar as for SARS-CoV-1 [13-16]. MERS-CoV (Gardner et al. [17] and influenza or similar viruses' outbreaks [4,7,8].

We can hypothesizes how the weather impact on the incidence of SARS-CoV-2 is linked to mood in the population. Bassi [60] concluded that bad weather caused worse mood in most of the population and is linked e.g. with lower interest for voter turnout in elections. Similarly, good mood was associated with lower humidity [61], high levels of solar radiation [62], high barometric pressure [63] and high temperatures [64]. The effect of solar radiation was strongest in spring [65].

SARS-COV-2 during weather with neutral circulation in mid-lattitudes: During decline NAO index from values above 1.0 under -1.0 (neutral phase of NAO, AO respectively), are visible in figure 2 and figure 3 signs of beginning polar vortex drop – correlations PP with incidence SARS-CoV-2 is even stronger such in NAO- equivalent above British Isles, area of Genoa cyclogenesis, Scandinavia and Baltic, but vortex is not dropped to the southern regions yet. Higher RR starts have less positive (or clearly negative) effect on incidence in Stormtrack Area and Mediterranean and SS and weaker wind starts have less negative effect. Higher temperatures and diurnal temperature range are not as bad as during NAO+/AO+. Cyclogenesis in Genoa area is strong, and RR can be more unfavorable than near NAO-.

SARS-COV-2 during predominant cyclonic weather (NAO-/AO-, AO neutral respectively) in the mid-latitudes: It appears that NAO-/AO- phases play an important part in the weakening effect of drought on the incidence of SARS-CoV-2 during spring, summer and autumn. Although in winter this weather is linked with big coldwaves and lower temperatures are significantly linked with higher incidence in Western, Central Europe and larger part of Iberian Peninsula precipitation, humidity and cloudiness which NAO-/AO- brings to mid- and subtropical latitudes have substantial effect on the decreasing of the number of diagnosed SARS-CoV-2 cases.

During the low-pressure pattern above mid-latitudes (figure 2 and figure 3, the entire column for 0-9 day

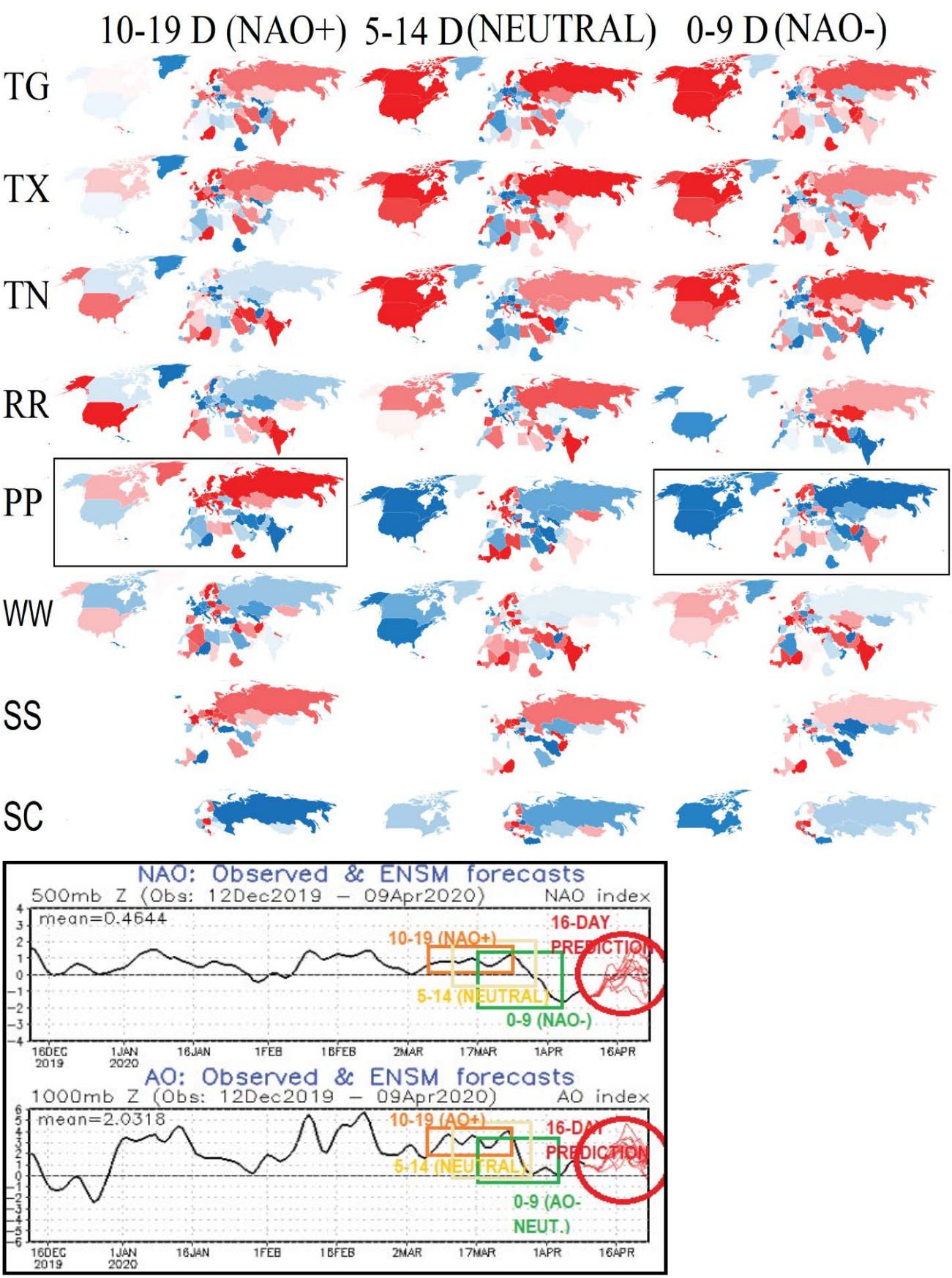

Figure 3: Up: Average correlation coefficients from table 2/figure 2 for all countries and dependent territories. In a rectangle averages for PP during 1st period of incubation time (0-9 days before an incidence) corresponding to NAO-/AO- or AO neutral phase respectively an 3rd period of incubation time (10-19 days before an incidence) corresponding to NAO+/AO+ phase (Basemap © Geonames, MSFT); Down: NAO and AO index during winter 2019/2020 and early spring 2020. Investigated 3 periods of incubation time during early spring 2020 are marked with rectangles, prediction with red circle.

(NAO-)), lower pressure, higher wind and less than NAO+ lower precipitation, higher sunshine and higher diurnal temperature range (mainly higher maximum temperatures) above mid-latitudes were unfavorable. The effect of negative PP is widely spread across all regions, except for parts of Arctic and Scandinavia (Greenland height), RR starting to be more unfavorable and higher SS and weaker WW more favorable with comparison with NAO+. SC is appearing in Europe and is linked with higher incidence (and cold weather(!)). Lower temperatures are more unfavorable for higher incidence of SARS-CoV-2, mainly in western half of Europe. We can therefore certify favorable effect of PP and temperatures on the virus' incidence both in Eastern half of Europe and eastern regions during NAO-/AO-.

On the pages https://www.cpc.ncep.noaa.gov/products/precip/CWlink/pna/nao.shtml and https://www.cpc.ncep.noaa.gov/products/precip/CWlink/daily_ao_index/ao.shtml we can monitor daily evolution of NAO and AO index. There are available 16-day predictions of indices, which can help to estimate the impact of main phases of circulation conditions on increase/decrease of incidence SARS-C_0V-2 during seasons in 2020 and next years. Evolution of NAO and AO index during winter 2019/2020 and early spring 2020 contains figure 3. Investigated 3 periods of incubation time during early spring 2020 and 16-day prediction are marked here.

Regarding the findings of Bukhari and Jamel, [5,6,9-11,13]. we are suggesting that the observed unfavorable cooling effect of temperature on the incidence of SARS-CoV-2 can be weakened by better mood and more spending leisure time outside during the sunny, warm, anticyclonic weather [14,60-64]. This effect can be amplified by strong solar radiation in the spring [65]. This effect can be especially strong in the case of SARS-CoV-2, when pandemics is widely spread, and people have to carefully choose when they can afford to use their time to stay outdoors.

NCEP/NCAR Reanalysis comparison with 3 incubation time periods

Computed NCEP/NCAR Reanalysis plots for identified positive, negative and neutral phase of NAO/AO during incubation time periods in figure 2 and 3 were verified and plotted for better understanding of circulation conditions of period before substantial outbreak of SARS-CoV-2.

In figure 4 we can refer to conditions during individual 3 phases of incubation time/NAO. At maps of H500 we can see weakening of polar vortex (from NAO+ to NAO- phase) – Azores height and Icelandic Low both. Domain of low pressure above Arctic is weakened and low geopotential is dropped to Mediterranean. RH850 shows dropped zone of higher relative humidity from northern mid-latitudes during NAO+ to Mediterranean during NAO-, while in northern regions relative humidity decreased. T850 immediately responds to drop of polar vortex and zone with lower temperatures fast covers mid-latitudes in Europe and parts of Mediterranean. Zonal and meridional flow (U-winds and W-winds) are weakened across northern and southern latitudes both.

Simultaneous same and opposite effects of meteorological elements

Finally, we have made correlation matrixes between effects of 8 meteorological elements on the incidence of SARS-COV-2, every with each other. This output is computed for 13 partial regions, separately (Table 3). Relationships significant at level 0.10 were given to the maps (Figure 5).

We can confirm bigger connections between variables (Table 3) derived from table 2 in the most affected main regions with the biggest rate of statistically significant responses – mainly Western Europe Western Mediterranean and Balkan, Arctic and Central Europe too. In the regions, where pandemics started to spread later, or incidence rates were low (mainly southern tropical, or Asian regions, Eastern Europe eventually) are relationships between variables and overall amount of statistically significant responses is lower.

It is interesting that in Arctic almost all variables are linked with same simultaneous shift, while in Western Europe, Western Mediterranean and Balkan were identified relative strong opposite simultaneous shifts of variables. It shows that in Arctic (or the most northern regions) could be conditions for outbreaks of SARS-CoV-2 relatively fast improved or worsened, while in southern regions are working negative feedbacks trying to autoregulate and stabilize conditions of spreading of virus. Conditions in Arctic can be linked with Arctic Amplification feedback and general shift of all meteorological elements the same way [66-69].

It appears that in the same shift act PP and SS with TG; PP, SS and WW with TX; PP, RR and WW with TN – mainly during NAO- phase; temperatures, WW and SC with RR – mainly during NAO+ phase; temperatures and SS with PP; temperatures, SS and RR during NAO+/NAO- phases both strongly; temperatures, WW and PP with SS – mainly during NAO- phase and WW, RR with SC. Opposite simultaneous effect is more common in favor NAO- phase with blue NAO- signs : red NAO+ symbols on figure 5 ratio 36:24.

It appears totally averse effect act RR, PP, WW and SC with TG and TX – mainly during NAO- phases; PP, WW and SS with TN – during NAO+ and NAO- phases both; temperatures, PP, WW and SS with RR during NAO+ and NAO- both; temperatures, RR and WW with PP – mainly during NAO+; temperatures, RR, PP, SS with WW; temperatures, RR, WW and SC with SS – mainly during NAO- phases and temperatures, PP and SS with SS – mainly during NAO- phases. Opposite simultaneous effect is more common in favor NAO- phase, again with of NAO- : NAO+ symbols on figure 5 ratio 47:29 [70,71].

This means that during NAO- are relationships between variables stronger and that opposite effects are more common than same effects, what can lead to autoregulation.

Discussion and Conclusion

This analysis provides evidence of an environmental component contributing to the development of SARS-COV-2 infections. We investigated the effect of 8 meteorological elements on the incidence of SARS-COV-2 during 3 periods

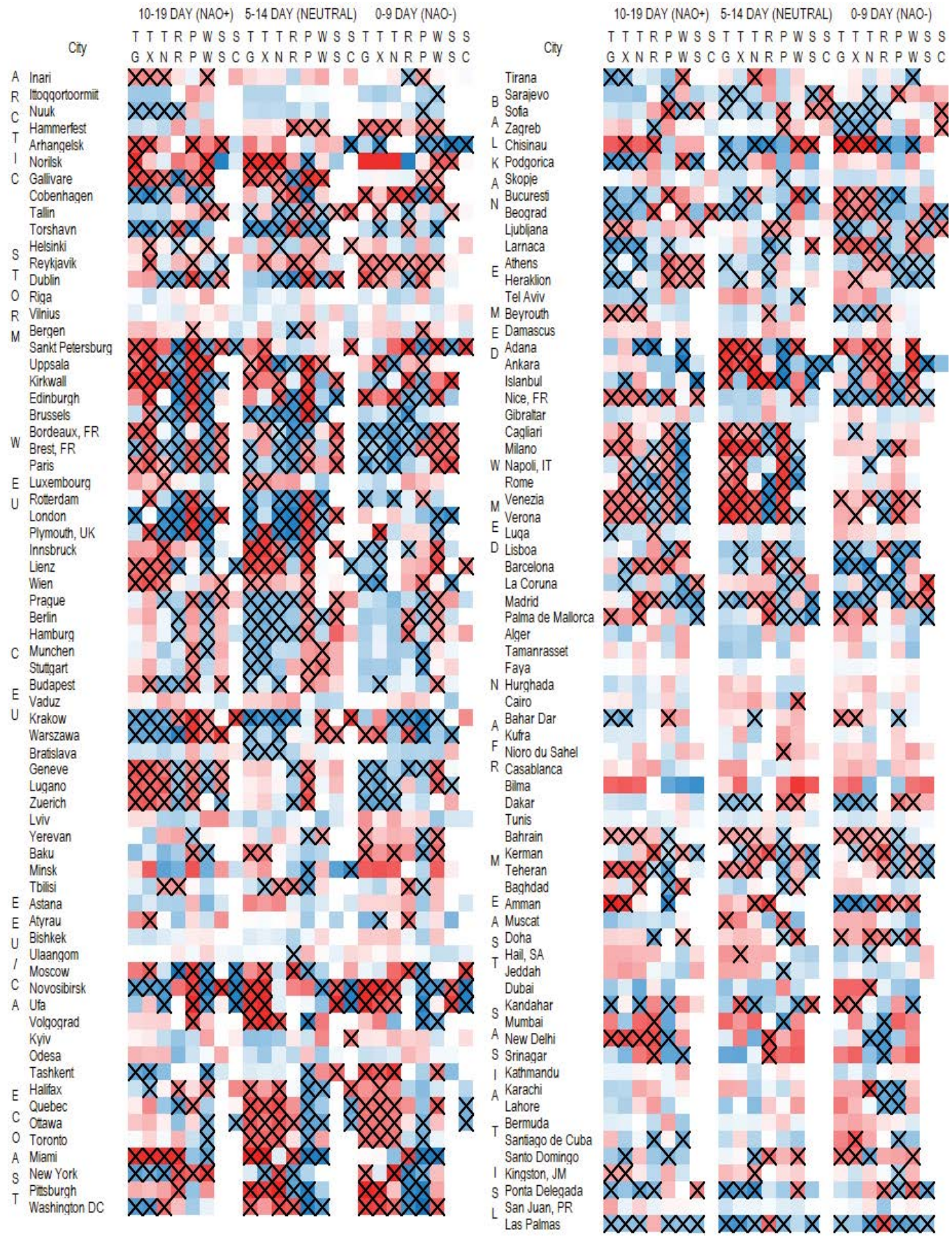

Table 2: Spearman correlation ranks between daily means of 8 meteorological elements (average temperature (°C), TX – maximum temperature (°C), TN – minimum temperature (°C), RR – 24-hours precipitation (mm), PP – air pressure (Hpa), WW – average daily wind speed (km/h), SS – sunshine duration (h) and snow cover (cm)) and daily incidence of SARS-COV-2 for 3 incubation time periods (1st 0-9 day/NAO-; 2nd 5-14 day/NAO neutral; 3rd 10-19 day/NAO+) and circulation phases in 137 cities. Crossed cells – significant at level 0.10.

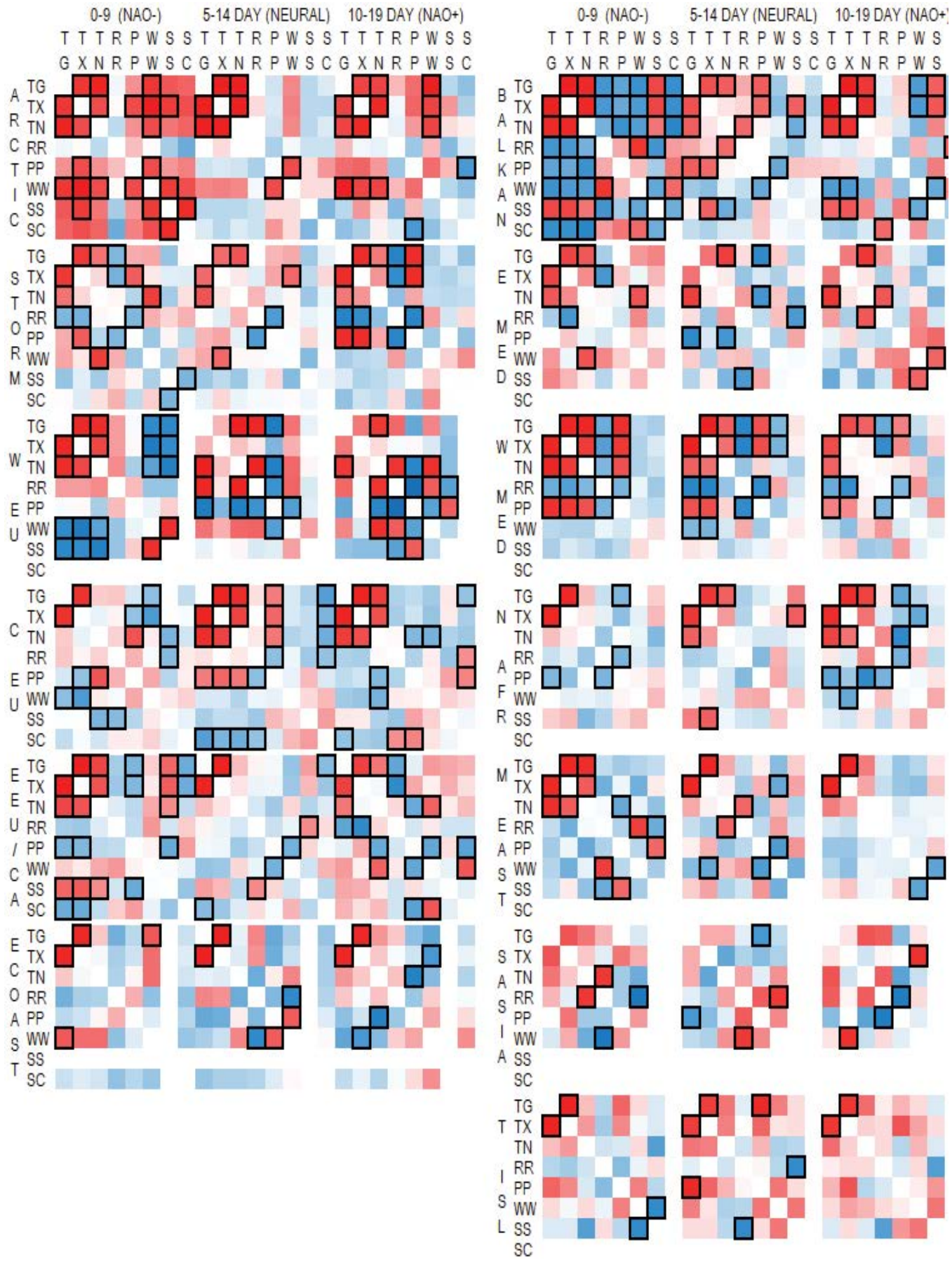

Table 3: Correlation matrixes (Spearman correlation rank) between impacts of 8 meteorological elements on the incidence of SARS-COV-2 every with each other. This output is computed for 13 partial regions and for all 137 stations (All set), separately and 3 incubate time periods (such in figure 3). Statistically significant responses at level 0.10 are in frames.

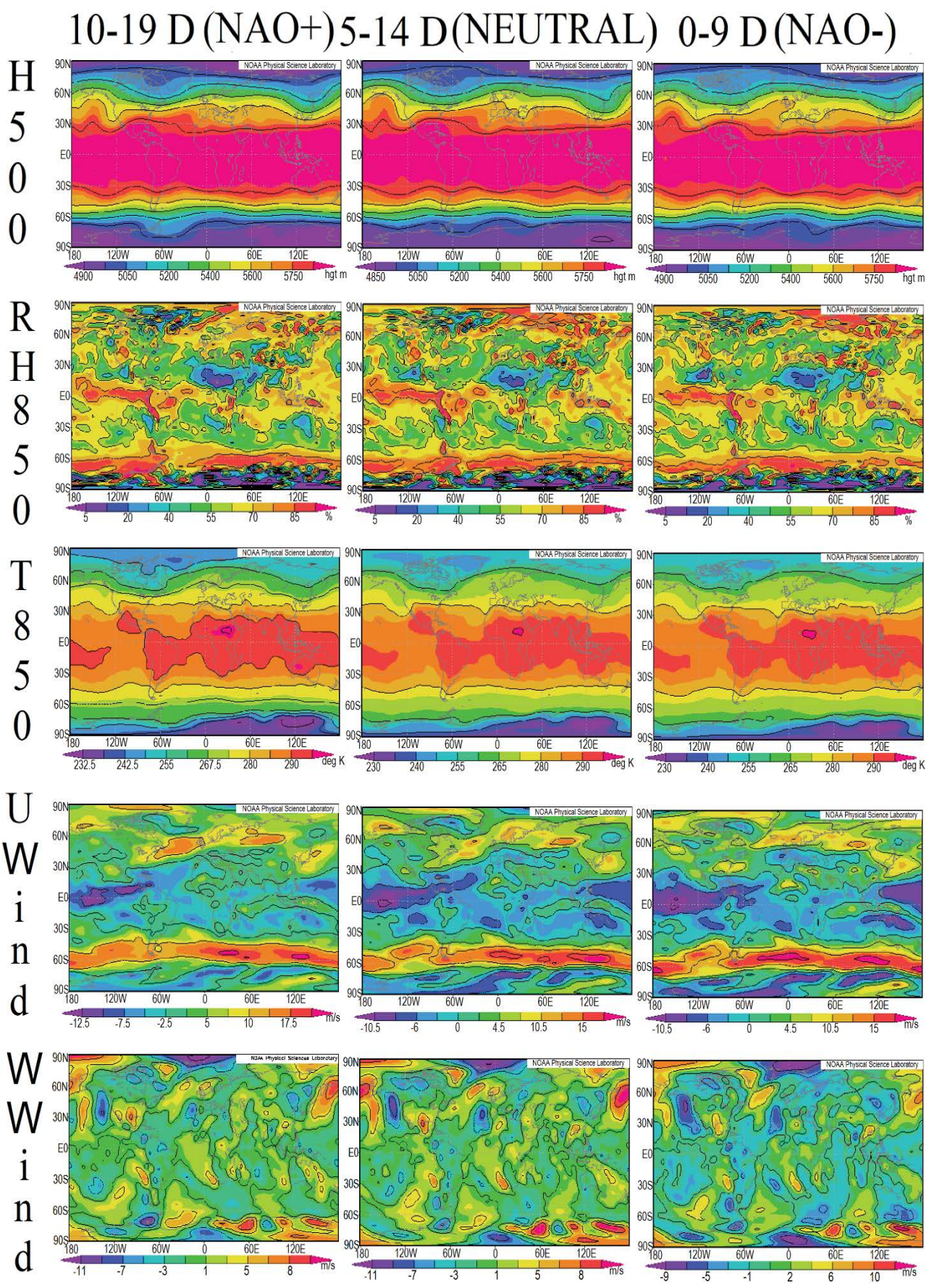

Figure 4: NCEP/NCAR Reanalysis for 3 incubation time periods of SARS-CoV-2 (same as in **Fig. 3**). H500: geopotential height at level 500 Hpa; RH850: relative humidity at level 850 hPa; T850: temperature at level 850 hPa; U wind/Wwind: zonal/meridional winds at level 850 hPa (plotted from NCEP/NCAR Reanalysis, Physical Sciences Laboratory NOAA).

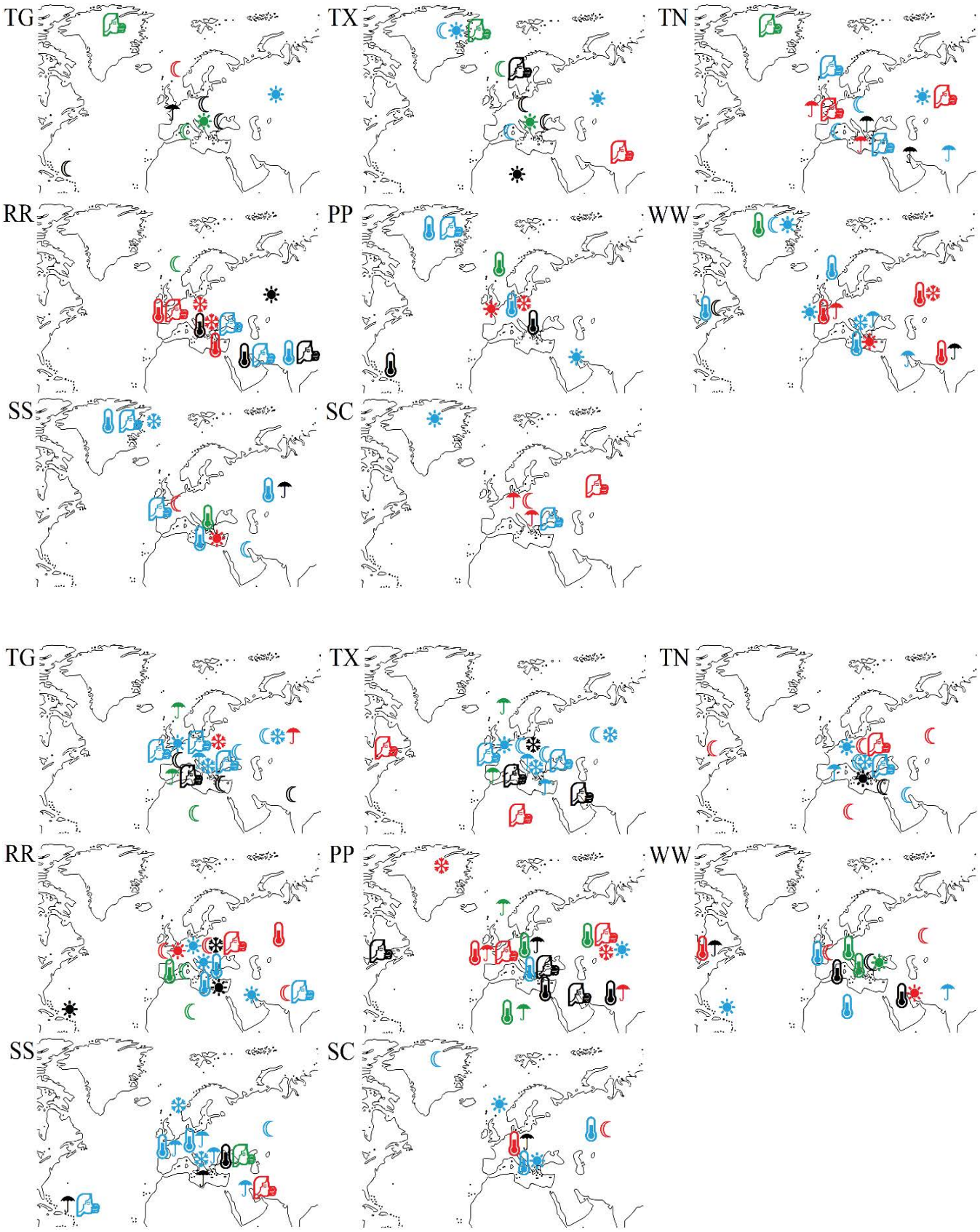

Figure 5: Spearman correlation ranks from table 3 significant at level 0.10 given to the schematic maps (up – positive correlations set, down – negative correlations set). □□ symbol used for all TG, TX, TG; ☂ for RR; ☾ for PP; □ for WW; ☀ for SS and ❄ for SC. Blue symbols for NAO- or NAO- and neutral, black symbols for neutral, green for NAO+ and NAO- both (or in addition neutral) and red for NAO+ or NAO+ and neutral phase.

of incubation time of the virus corresponding with main circulation patterns in mid-latitude areas in Europe and its wider region during early spring 2020.

Results suggest that incidence of SARS-COV-2 can depends on main circulation patterns in Euro-Atlantic or Northern Hemisphere region, respectively, linked with high-, neutral and low- pressure zones above mid-latitudes. Results have shown that, during the high-pressure pattern above mid-latitudes, lower precipitation, higher pressure, weaker wind, higher sunshine, higher diurnal temperature range (higher maximum and lower minimum temperatures) were very unfavorable for incidence of SARS-CoV-2 (more cases) and that, during the low-pressure pattern above mid-latitudes, lower pressure, higher wind and less than NAO+ lower precipitation, higher sunshine and higher diurnal temperature range (mainly higher maximum temperatures) were unfavorable. For comparison these results with circulation conditions NCEP/NCAR reanalysis were outputted.

We agree with previous findings suggesting that incidence SARS-CoV-2 is higher during drought (and low humidity and precipitation) or higher diurnal temperature range [5,6,9-11,13,14]. Results regarding dry conditions are very similar as for SARS-CoV-1 [13-16] MERS-CoV [17] and influenza or similar viruses' outbreaks [4,7,8]. We have added to the list of unfavorable meteorological elements the following options.

The weather impact on the incidence of SARS-CoV-2 can be linked to mood in the population [60]. Mainly NAO+ phases are associated with lower humidity [61], high levels of solar radiation [62], high barometric pressure [63] and high temperatures [64]. The effect of solar radiation was strongest in spring [65], which can negatively affect incidence in April and May 2020. We are suggesting that the observed unfavorable cooling effect of temperature on the incidence of SARS-CoV-2 can be weakened by better mood and more spending leisure time outside during the sunny, warm, anticyclonic weather.

For better understanding, simultaneous effects of meteorological elements were investigated. During NAO+, precipitation and wind/minimum temperatures, precipitation and pressure; during NAO- phase minimum temperatures, wind and sunshine/maximum, minimum and average temperatures, precipitation, sunshine and snow cover have the most simultaneous same/opposite effects.

References

1. WHO (2020a) Statement on the second meeting of the International Health Regulations (2005) Emergency Committee regarding the outbreak of novel coronavirus (2019-nCoV). World Health Organization.
2. WHO (2020b) WHO Director-General's opening remarks at the media briefing on SARS-COV-2-11 March 2020. World Health Organization.
3. Iacobucci G (2020) Sixty seconds on . . . anosmia [loss of smell]. BMJ 368: m1202.
4. Harmooshi N, Shirbandi K, Rahim F (2020) Environmental Concern Regarding the Effect of Humidity and Temperature on SARS-COV-2 (SARS-COV-2) Survival: Fact or Fiction. SSRN.
5. Bukhari Q, Jameel Y (2020) Will Coronavirus Pandemic Diminish by Summer? SSRN.
6. Sajadi, MM, Habibzadeh P, Vintzileos A, Shokouhi S, Miralles-Wilhelm F, et al. (2020) Temperature, Humidity and Latitude Analysis to Predict Potential Spread and Seasonality for SARS-COV-2. JAMA Netw Open 3: e 2011834.
7. Tang JW (2009) The effect of environmental parameters on the survival of airborne infectious agents. J R Soc Interface 6: S737-S746.
8. Lowen AC, Steel J (2014) Roles of humidity and temperature in shaping influenza seasonality. J Virol 88: 7692-7695.
9. Wang, J, Tang K, Feng K, Weifeng L (2020) High Temperature and High Humidity Reduce the Transmission of SARS-COV-2. SSRN.
10. Ma Y, Zhao Y, Liu J, He X, Wang B, et al. (2020) Effects of temperature variation and humidity on the death of SARS-COV-2 in Wuhan, China. Science of the Total Environment 724: 138226.
11. Chan KH, Peiris JS, Lam SY, Poon LL, Yuen KY, et al. (2020) The Effects of Temperature and Relative Humidity on the Viability of the SARS Coronavirus. Adv Virol.
12. Xiao W, Nethery RC, Sabath BM, Braun D, Dominici D (2020) Exposure to air pollution and SARS-COV-2 mortality in the United States. medRxiv.
13. Araujo MB, Naimi B (2020) Spread of SARS-CoV-2 Coronavirus likely to be constrained by climate. medRxiv.
14. Brassey J, Heneghan C, Mahtani K R, Aronson J K (2020) Do weather conditions influence the transmission of the coronavirus (SARS-CoV-2)?. The Centre for Evidence-Based Medicine.
15. Lin K, Yee-Tak Fong D, Zhu B, Karlberg J (2006) Environmental factors on the SARS epidemic: air temperature, passage of time and multiplicative effect of hospital infection. Epidemiol Infect 134: 223-230.
16. Tan J, Mu L, Huang J, Yu S, Chen B, et al. (2005) An initial investigation of the association between the SARS outbreak and weather: with the view of the environmental temperature and its variation. Journal of Epidemiology and Community Health 59: 186-192.
17. Gardner EG, Kelton D, Poljak Z, Van Kerkhove M, von Dobschuetz S, et al. (2019) A case-crossover analysis of the impact of weather on primary cases of Middle East respiratory syndrome. BMC Infect Dis 19: 113.
18. Tirupathi R, Ramparas TR, Wadhwa G, Areti S, Kaur J, et al. (2020a) Viral dynamics in the Upper Respiratory Tract (URT) of SARS-CoV-2. Infez Med 28: 486-499.
19. Kim ES, Chin BS, Kang CK (2020) Clinical course and outcomes of patients with severe acute respiratory syndrome coronavirus 2 infection: a preliminary report of the first 28 patients from the Korean Cohort Study on COVID-19. J Korean Med Sci 35: e142.
20. Liu Y, Yan LM, Wan L (2020) Viral dynamics in mild and severe cases of COVID-19. Lancet Infect Dis 20: 656-657.
21. Li G, Ling L, Lai CK (2020) Viral dynamics of SARS-CoV-2 across a spectrum of disease severity in COVID-19. J Infect 81: 318-356.
22. Zheng S, Fan J, Yu F (2020) Viral load dynamics and disease severity in patients infected with SARS-CoV-2 in Zhejiang province, China, January-March 2020: retrospective cohort study. BMJ 369.
23. Xu K, Chen Y, Yuan J (2020) Factors associated with prolonged viral RNA shedding in patients with coronavirus disease 2019 (COVID-19). Clin Infect Dis 71: 799-806.
24. Weisblum Y, Schmidt F, Zhang F (2020) Escape from neutralizing antibodies by SARS-CoV-2 spike protein variants. Elife 9:e61312.
25. Bunyavanich S, Do A, Vicencio A (2020) Nasal gene expression of angiotensin-converting enzyme 2 in children and adults. JAMA. 323: 2427-2429.
26. Tirupathi R, Bharathidasan K, Palabindala V, Salim SA, Al-Tawfiq JA (2020b) Comprehensive review of mask utility and challenges during

the COVID-19 pandemic. Infez Med 28(suppl 1): 57-63.

27. WHO (2020c) Modes of transmission of virus causing COVID-19: implications for IPC precaution recommendations.

28. Santarpia JL, Rivera DN, Herrera V (2020) Transmission Potential of SARS-CoV-2 in Viral Shedding Observed at the University of Nebraska Medical Center. medRxiv.

29. Klompas M, Baker MA, Rhee C (2020) Airborne Transmission of SARS-CoV-2: Theoretical Considerations and Available Evidence. JAMA 324: 441-442.

30. Morawska L, Johnson GR, Ristovski ZD, Hargreaves M, Mengersen Ket al. (2009b) Size distribution and sites of origin of droplets expelled from the human respiratory tract during expiratory activities. J Aerosol Sci 40: 256-269.

31. Fennelly KP (2020) Particle sizes of infectious aerosols: implications for infection control. Lancet Respir Med 8: 914-924.

32. Ma QX, Shan H, Zhang HL, Li GM, Yang RM, et al. (2020b) Potential utilities of mask wearing and instant hand hygiene for fighting SARS-CoV-2. J Med Virol 92: 1567-1571.

33. Brosseau LM (2020) Are Powered Air Purifying respirators a solution for protecting healthcare workers from emerging aerosol-transmissible diseases? Ann Work Expo Heal 64: 339-341.

34. Bae S, Kim M, Kim JY (2020) Effectiveness of Surgical and Cotton Masks in Blocking SARS–CoV-2: A Controlled Comparison in 4 Patients. Ann Intern Med 173: W22-W23.

35. Morawska L, Tang JW, Bahnfleth W, Bluyssen PM, Boerstra A, et al. (2020) How can airborne transmission of COVID-19 indoors be minimised?. Environment International 142: 105832.

36. Yang W, Marr LC (2011) Dynamics of airborne influenza a viruses indoors and dependence on humidity. PLoS One 6: e21481.

37. Ming Hui CH, Cheng W, Goh SS, Kong J, Li B, et al. (2020) Face Masks in the New COVID-19 Normal: Materials, Testing, and Perspectives. Research.

38. Long Y, Hu T, Liu L (2014) Effectiveness of N95 respirators versus surgical masks against influenza: a systematic review and meta-analysis. Journal of Evidence-Based Medicine 13: 93-101.

39. Davies A, Thompson KA, Giri K, Kafatos G, Walker J Bennett A (2013) Testing the efficacy of homemade masks: would they protect in an influenza pandemic?. Disaster Medicine and Public Health Preparedness 7: 413-418.

40. Mueller AV, Eden MJ, Oakes JJ, Bellini C, Fernandez LA (2020) Quantitative method for comparative assessment of particle filtration efficiency of fabric masks as alternatives to standard surgical masks for PPE. Matter 3: 950-962.

41. van der Sande M, Teunis P, Sabel R (2008) Professional and home-made face masks reduce exposure to respiratory infections among the general population. PLoS One 3: e2618.

42. Rubbo SD, Abbott LR (1968) Filtration efficiency of surgical masks: a new method of evaluation. Australian and New Zealand Journal of Surgery 38: 80-83.

43. Chu DK, Akl EA, Duda S (2020) COVID-19 Systematic Urgent Review Group Effort (SURGE) study authors. Physical distancing, face masks, and eye protection to prevent person-to-person transmission of SARS-CoV-2 and COVID-19: a systematic review and meta-analysis. Lancet 395: 1973-1987.

44. O'Kelly E, Pirog S, Ward J, Carkson PJ (2020) Ability of fabric face mask materials to filter ultrafine particles at coughing velocity. BMJ Open 10: e039424.

45. Neupane BB, Mainali S, Sharma A, Giri B (2019) Optical microscopic study of surface morphology and filtering efficiency of face masks. Peer J 7: e7142-e7142.

46. Liu G, Nie J, Han C (2020b) Self-powered electrostatic adsorption face mask based on a triboelectric nanogenerator. ACS Applied Materials & Interfaces. 10: 7126-7133.

47. Ma S, Zhang M, Nie J, Yang B, Song S, et al. (2020c) Multifunctional cellulose-based air filters with high loadings of metal–organic frameworks prepared by in situ growth method for gas adsorption and antibacterial applications. Cellulose 25: 5999-6010.

48. Holme I (1999) Adhesion to textile fibres and fabrics. International Journal of Adhesion and Adhesives 19: 455-463.

49. Nathan N (2020) Waste Not, Want Not: The Re-Usability of N95 Masks. Anesth Analg 131: 3.

50. Volz E, Mishra V, Chand M, Barrett JC, Johnson R, et al. (2020) Transmission of SARS-CoV-2 Lineage B.1.1.7 in England: Insights from linking epidemiological and genetic data - The COVID-19 Genomics UK (COG-UK) consortium, Seth Flaxman, Oliver Ratmann, Samir Bhatt, Susan Hopkins, Axel Gandy, Andrew Rambaut, Neil M Ferguson. medRxiv.

51. Liu Y, Gayle AA, Wilder-Smith A, Rocklöv J (2020c) The reproductive number of COVID-19 is higher compared to SARS coronavirus. J Travel Med 27: taaa021.

52. Hurrell JW, Kushnir Y, Ottersen G, Visbeck M (2003) An overview of the North Atlantic Oscillation. The North Atlantic Oscillation: Climatic Significance and Environmental Impact, Geophysical monograph. American Geophysical Union, Washington, DC.

53. Hurrell JW (1995) Decadal trends in the North Atlantic oscillation: Regional temperatures and precipitation. Science 269: 676-679.

54. Hurrell JW, Desser C (2009) North Atlantic climate variability: The role of the North Atlantic Oscillation. Journal of Marine Systems 78: 28-41.

55. Hurrell JW, Van Loon H (1997) Decadal variations in climate associated with the North Atlantic Oscillation. Clim. Change 36: 301-326.

56. Kapala AH, Machel H, Flohn H (1998) Behaviour of the centres of action above the Atlantic since 1881. Part II: Associations with regional climate anomalies. Int J Climatol 18: 23-36.

57. Wanner H, Bronninmann S, Casty C, Gyalistras D, Luterbacher J, et al. (2001) North Atlantic oscillation - Concepts and studies. Surveys in Geophysics. 22: 321-382.

58. Blade I, Liebmann B, Fortuny D (2012) Observed and simulated impacts of the summer NAO in Europe: implications for projected drying in the Mediterranean region. Clim Dyn 39: 709-727.

59. Boé J, Terray L, Cassou C, Najac J (2008) Uncertainties in European summer precipitation changes: role of large scale circulation. Clim Dyn 33: 265-276.

60. Bassi A (2013) Weather, Mood, and Voting: An Experimental Analysis of the Effect of Weather Beyond Turnout. SSRN.

61. Sanders JL, Brizzolara MS (1982) Reand Mood. Journal of General Psychology 107: 155-156.

62. Parrot GW, Sabini J (1990) Mood and Memory under Natural Conditions: Evidence for Mood Incongruent Recall. Journal of Personality and Social Psychology 59: 321-336.

63. Goldstein KM (1972) Weather, Mood, and Internal-External Control. Perceptual Motor Skills 35: 786.

64. Cunnigham M R (1979) Weather, Mood, and Helping Behavior: Quasi-experiments with Sunshine Samaritan. Journal of Personality and Social Psychology 37: 1947-1956.

65. Keller MC, Fredrickson BL, Ybarra O, Côté S, Johnson K, et al. (2005) A Warm Heart and a Clear Head. The Contingent Effects of Weather on Mood and Cognition. Psychological Science 16: 724-731.

66. Budikova D (2009) Role of Arctic sea ice in global atmospheric circulation: A review. Global and Planetary Change 68: 149-163.

67. Petoukhov V, Semenov V (2010) A link between reduced Barents-Kara sea ice and cold winter extremes over northern continents. J Geophys

Res Atmos 115.

68. Francis JA, Vavrus SJ (2012) Evidence linking Arctic amplification to extreme weather in mid-latitudes. Geophys Res Lett 39: L06801.

69. Walsh JE (2014) Intensified warming of the Arctic: Causes and impacts on middle latitudes. Global and Planetary Change Volume 117: 52-63.

70. Biggerstaff M, Cauchemez S, Reed C (2014) Estimates of the reproduction number for seasonal, pandemic, and zoonotic influenza: a systematic review of the literature. BMC Infect Dis14: 480.

71. Sanche S, Lin YT, Xu C, Romero-Severson E, Hengartner N, et al. (2020) High contagiousness and rapid spread of severe acute respiratory syndrome coronavirus 2. Emerg Infect Dis 26: 1470-1477.